Genetic and epigenetic reprogramming in response to internal and external cues by induced transposon mobilization in Moso bamboo

Long-Hai Zou[1,*], Bailiang Zhu[1,*], Yaxin Chen[1], Yaping Lu[1], Muthusamy Ramkrishnam[2], Chao Xu[1], Xiaohong Zhou[1],Yiqian Ding[1], Jungnam Cho[3,†], Mingbing Zhou[1,†]

[1]State Key Laboratory of Subtropical Silviculture, Bamboo Industry Institute, Zhejiang A&F University, Hangzhou, Zhejiang, China.

[2]State Key Laboratory of Tree Genetics and Breeding, Co-Innovation Center for Sustainable Forestry in Southern China, Bamboo Research Institute, Key Laboratory of National Forestry and Grassland Administration on Subtropical Forest Biodiversity Conservation, College of Biology and the Environment, Nanjing Forestry University, Nanjing 210037, Jiangsu, China

[3]Department of Biosciences, Durham University, Durham DH1 3LE, United Kingdom.

*These authors contributed equally to this work.

†e-mail: zhoumingbing@zafu.edu.cn; jungnam.cho@durham.ac.uk

Summary

- Long terminal repeat retroelements (LTR-REs) have profound effects on DNA methylation and gene regulation. Despite the vast abundance of LTR-REs in the genome of Moso bamboo (*Phyllostachys edulis*), an industrial crop in under-developed countries, their precise implication of the LTR-RE mobility in stress response and development remains relatively unknown.
- We investigated the RNA and DNA products of LTR-REs in Moso bamboo at various developmental stages and stressful conditions. To our surprise, our analyses identified thousands of active LTR-REs, in particular from those that are proximal to genes involved in stress response and developmental regulation. These genes adjacent to active LTR-REs exhibited an increased expression under stress and are associated with reduced DNA methylation that is likely affected by the induced LTR-REs.
- Moreover, the analyses of simultaneous mapping of insertions and DNA methylation showed that the LTR-REs effectively alter the epigenetic status of the genomic regions where they inserted, and concomitantly their transcriptional competence which might impact the stress resilience and growth of the host.
- Our work unveils the unusually strong LTR-RE mobility in Moso bamboo and its close association with (epi)genetic changes, which supports the co-evolution of the parasitic DNAs and host genome in attaining stress tolerance and developmental robustness.

Keywords: ALE-seq; eclDNA; LTR retrotransposons; DNA methylation; *Phyllostachys edulis*; RNA-seq

Introduction

Long terminal repeat retroelement (LTR-RE) is a kind of transposons ubiquitous in eukaryotic genomes and the most abundant genomic components particularly in flowering plants. LTR-REs can autonomously colonize the host genomes in a copy-paste manner via RNA intermediates forming new copies. A typical intact LTR-RE contains two identical LTRs at both ends, a primer binding site (PBS) following the 5' LTR, a polypurine tract (PPT) preceding the 3' LTR, and between the PBS and PPT, two internal coding regions for a nucleocapsid (*gag*) and a polyprotein (*pol*) (Kumar & Bennetzen, 1999). PBS and PPT are the sites that initiate reverse transcription of extrachromosomal linear DNA (eclDNA) of the minus and plus strand, respectively. The *gag* gene encodes a virus-like particle (VLP) protein that encapsulates the transposon RNA-nucleocapsid complex for reverse transcription. The *pol* gene products include protease (PR), reverse transcriptase (RT), RNase H (RH) and integrase (IN), all of which are essential for the synthesis of eclDNAs and their integration into the host genome. In short, an LTR-RE copies to a new genomic locus by inserting the eclDNA that is reverse transcribed from the cognate RNA transcript.

Despite the mobile nature of transposons in the host genome, their essential role and significance pertain to the regulation of gene expression (Comfort, 1999). Specifically, the impact of LTR-REs varies from serving as promotors/cis-elements to inducing alternative splicing and providing premature termination sites through signals conveyed by insertions (Grandbastien, 2015). For example, an LTR-RE *MT2B2* in mammals acts as an alternative promoter to drive the expression of a *CDK2AP1* isoform, which controls the timing of pre-implantation development (Modzelewski *et al.*, 2021; Canat & Torres-Padilla, 2021). In soybean, the insertion of a Ty1-*Copia* LTR-RE within the first exon of a phytochrome A paralog results in the creation of a stop codon, which in turn produces a truncated protein that causes insensitivity to long day flowering (Liu *et al.*, 2008; Kanazawa et al., 2009). Apart from these, LTR-REs can influence the expression of the host genes by altering epigenetic regulation. In rice tissue culture, the demethylation of LTR-RE *Tos17* was observed to extend into some flanking genomic regions (Liu *et al.*, 2004). Particularly, the reduced methylation of LTR-REs is correlated with an increase of expression levels of their adjacent genes (Huettel et al., 2006).

To maintain the stability and integrity of host genome, LTR-REs are usually silenced primarily by the host's epigenetic mechanism (Huettel et al., 2006). Despite the innate and tight suppression, many studies have shown that transposons can be activated at both transcriptional and transpositional levels by environmental challenges and intrinsic factors such as heat and phytohormones. For examples, the transcription of *OARE-1* (*Oat retroelement-1*) retrotransposon from *Avena sativa* is strongly induced by jasmonic acid and ultraviolet (UV) radiation (Kimura et

al., 2001) and *Onsen* from *Arabidopsis thaliana* produces a high level of RNA and eclDNA under heat shock (Matsunaga et al., 2011). *In vitro* tissue culture is deemed a stressful condition for plant cells due to its fluctuating micro-environment and is known to trigger vast genetic and epigenetic alterations (Ghosh et al., 2021). It is well documented that LTR-REs can be reactivated during callus culture; for instance, *Tos17* of rice is eruptible in transcripts and DNA copies by callus culture (Hirochika et al., 1996; Lanciano et al., 2017). In addition to stress treatments, LTR-REs can be released from epigenetic silencing in specific developmental stages. For example, massive retrotransposons are de-repressed in the shoot apical meristem at the juvenile stage (Gutzat et al., 2020) and vegetative cells of male gametophytes of *A. thaliana* (Martínez & Slotkin, 2012). However, our knowledge of the inherent significance of the temporal LTR-REs reactivated by stress and development is still incomplete, particularly in the non-model or orphan plant species.

Studies utilizing the model plants have detected only a limited number, or even a lack, of transposition events under stress or tissue culture (Sabot et al., 2011; Jiang et al., 2011; Miyao et al., 2011; Galindo-González et al., 2017), which restricted the investigation of functional roles of LTR-REs in response to external or internal challenges. This might be attributed to their relatively lower content of transposons and tight control by the host's epigenetic pathways. Conversely, the non-model plants with higher content of transposons and larger genomes may reserve a more frequent transposition events and thus provide us with the opportunities to study transposon-gene interaction (Grandbastien, 2015; Galindo-González et al., 2017). Detection of transposition events of LTR-REs has also been limited in classical methods such as transposon display, which can only reveal copy number variations of individual elements (Tsukahara et al., 2009; Ewing et al., 2015; Lanciano et al., 2017). Fortunately, several new methods have been developed recently, such as extrachromosomal circular DNA sequencing (Lanciano et al., 2017), sequence-independent retrotransposon trapping (SIRT) (Griffiths et al., 2018), and amplification of LTR of eclDNAs followed by sequencing (ALE-seq) (Cho *et al.*, 2018). Among these methods, ALE-seq is a high-throughput sequencing method that captures eclDNAs of activated LTR-REs, which is better suited for genomes with larger size and greater number of retrotransposons (Cho et al., 2018).

Moso bamboo (*Phyllostachys edulis*; synonym: *P. heterocycla*), the most economically valuable bamboo in China and Southeast Asia (Ramakrishnan et al., 2020), has a large genome of around two gigabases, LTR-REs of which occupy approximately 43.89% (Zhou *et al.*, 2017). Multiple active and full-length LTR-REs have been identified in Moso bamboo that was subjected to abiotic stresses. The LTR-RE *Phyllostachys heterocycla retrotransponson 9* (*PHRE9*) can be reactivated under radiation, cold, heat, and DNA methylation inhibitor treatments (Zheng et al., 2019). *PHRE1* and *PHRE2* are also activated by external environmental stimuli, such as high and

low temperatures and salt stress, and were able to transpose when transformed into *Arabidopsis thaliana* (Zhou et al., 2018). Moreover, our previous studies suggested that LTR-REs in Moso bamboo are abundantly present in the promoter regions of coding genes (Zhou *et al.*, 2017) and have much stronger transpositional activity than those in the model plants like rice and Arabidopsis (Zhou et al., 2017a). Hence, the Moso bamboo genome might serve as a better model to explore the interplay between LTR-REs and the host genes, particularly in the context of external and internal challenges.

The aim of this study is to identify the active LTR-REs and understand how they impact the host genome under stress and during development in Moso bamboo. Firstly, ALE-seq and RNA-seq were coupled to uncover the LTR-REs with both transcriptional and transpositional potential. Secondly, whole-genome bisulfite sequencing (WGBS) was applied to profile the methylome of those potentially active LTR-REs under the same conditions. Thirdly, transposon display technique was used to detect the insertion sites of the selected LTR-REs. Finally, transgenic approaches of both *in situ* and *ex situ* were used to validate the transpositional ability of selected LTR-REs and parse their insertion preferences. This study provides valuable insights into the molecular mechanisms for transposon activation during development and stress response of Moso bamboo, and their biological impact relevant to the rewiring of gene regulatory network.

Materials and Methods

Plant materials and sample collection

Seeds from a single inbred Moso bamboo plant were germinated and nurtured as described in Papolu et al. (Ramakrishnan et al., 2022). Five-week-old seedlings were treated with different stresses as following (Fig. 1a): (a) heat stress (Heat) at 42 ℃ for six hours (Han et al., 2018) (b) cold stress (Cold) at 4 ℃ for sixteen hours (Ying et al., 2011); (c) UV radiation (UV) under a ultraviolet lamp (100 μW/cm^2) from 50 cm distance for two hours (Zhang & Chen, 2011); and (d) salt stress (Salt) by irrigating with 200 mM NaCl for three days (Xiao et al., 2013). The seedlings grown at 25 ℃ with water irrigation (Wa) were used as the control. The first three leaves from the top were collected for ALE-seq, RNA-seq, and qPCR analyses. Three independent seedlings were prepared for each treatment. Calli generated from immature embryos of Moso bamboo seeds were cultured in a medium containing 500 mg/L proline, 500 mg/L glutamine, 300 mg/L casein hydrolysate, 2 mg/L 2, 4-D, 0.1 mg/L zeatin, 30 g/L sucrose, and 8.0 g/L agar (Fig. 1c). Three independent calli were individually collected and used for RNA and DNA extraction.

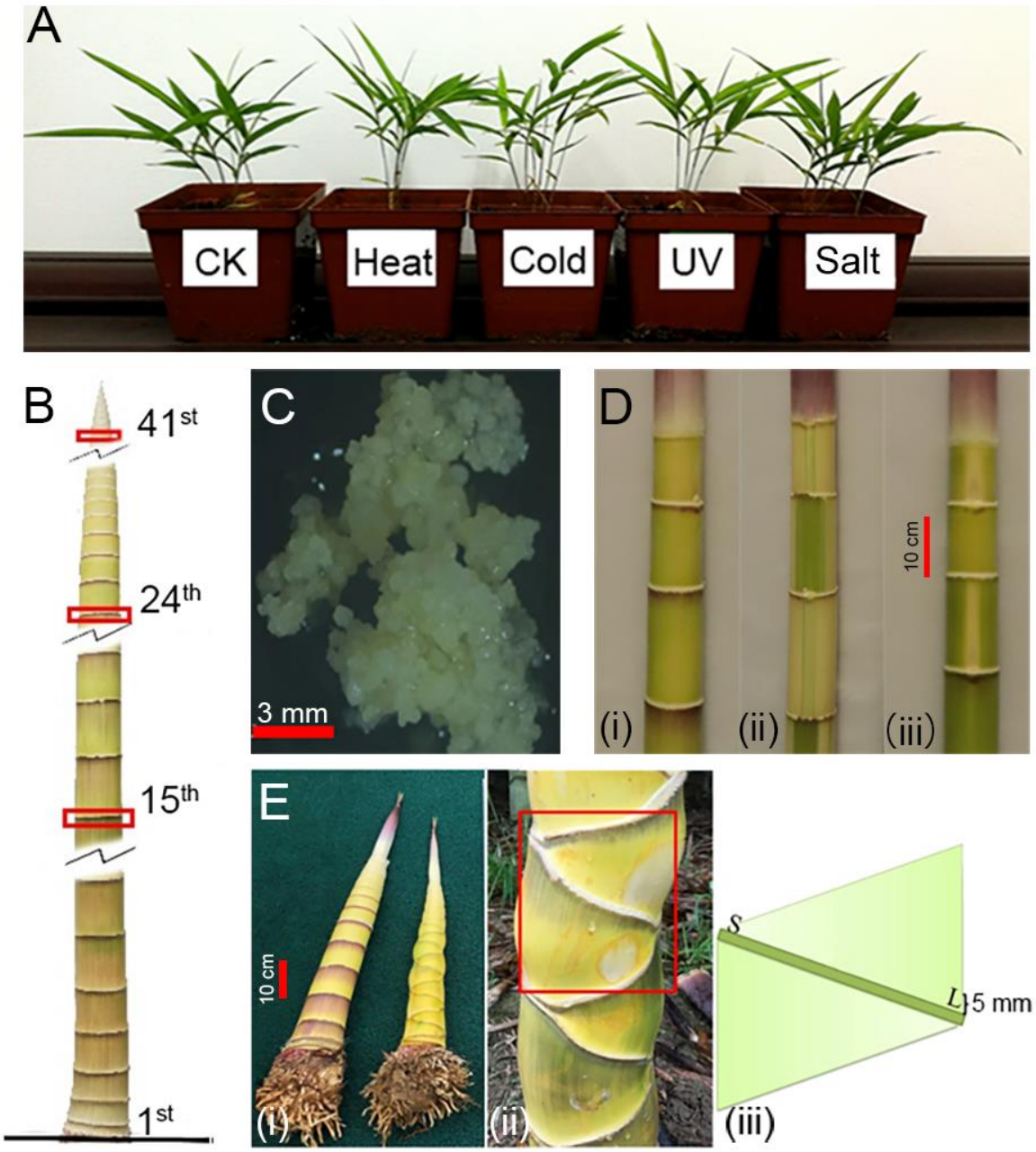

Fig. 1. Materials of Moso bamboo for capturing active LTR-REs. (a) Five-week-old seedlings that were treated with 42℃ (Heat), 0℃ (Cold), UV radiation, salt irrigation (Salt, NaCl). Control checks (CKs) were set synchronously. (b) A fast grown shoot shown the sampling internodes in the phases of initial cell division (ICD; 41st internode), rapid cell division (RCD; 24th internode treated as CK) and rapid cell elongation (RCE; 15th internode). (c) Calli generated from immature embryos. The presented calli had been cultured two months after induction. (d) The wild type of Moso bamboo (green internode, GI; i), *P. edulis* f. *viridisulcata* (green slot in internodes, GSI; ii) and *P. edulis* f. *luteosulcata* (yellow slot in internodes, YSI; iii). Intercalary meristems in internode slots during early coloring stage (24th internode) were sampled. (e) The wild type of Moso bamboo and *P. edulis* cv. *heterocycla*, a mutation type with tortoise-shell-like internodes (i). The red frame highlights tortoise-shell-like internodes in a shoot (ii). A sampling strategy diagram show that intercalary meristems in shrunk (IMS15) and lengthen (IML15) parts of 15th twisted internodes were collected (iii). Intercalary meristems form normal bamboo internodes (IMN15) were collected as controls. Three biological replicates were conducted on the above samples.

Moso bamboo plants were grown in the Cuizhu Garden of Zhejiang A&F and University, Hangzhou, China. Shoots of rapid growth stages were sampled at the 15th, 24th and 41st internodes (Fig. 1b), which corresponds to the phases of initiation of cell division (ICD), rapid cell division (RCD), and rapid cell elongation (RCE), respectively, as referenced in Tao et al. (2020).

The intercalary meristems in internode slots at the early coloring stages (24th internode) were sampled from two internode color variation types, *P. edulis* f. *luteosulcata* (yellow slot in internode, YSI) and *P. edulis* f. *viridisulcata* (green slot in internode, GSI), and the wild type of Moso bamboo (green internode, GI) (Fig. 1d). The intercalary meristems in shrunk (IMS15) and lengthen (IMS15) parts of the15th twisted internodes were sampled from an internode form mutation type (*P. edulis* cv. *heterocycla*) of Moso bamboo with tortoise-shell-like internodes (Fig. 1e). In the meantime, the corresponding tissues of the wild type Moso bamboo were collected as the control group. The internodes with color variation and form variation from three independent Moso bamboo shoots were sampled and subjected to ALE-seq and RNA-seq.

Identification and classification of LTR-REs

LTR-REs were identified with LTRpred (Drost, 2020) in the Moso bamboo genome published by Zhao et al. (Zhao et al., 2018). The parameters were set as "minlenltr=100, maxlenltr=5,000, mindistltr=4,000, maxdisltr=30,000, mintsd=3, maxtsd=20, vic=80, xdrop=7, motifmis=1, pbsradius=60, pbsalilen=c(8,40), pbsoffset=c(0,10), quality.filter=TRUE and n.orf=0". LTR-RE domain annotation was performed using LTRdigest (Steinbiss et al., 2009) with default settings. PBS motifs were also identified from the results of LTRdigest analysis. According to *gag* and *pol* coding regions, LTR-REs belonging to the *Gypsy* and *Copia* superfamilies were further classified into *tork*, *reftrofit*, *sire*, *oryco*, *del*, *reina*, *crm*, *tat*, *galadriel* and *athila* lineages (Llorens et al., 2007). The ratio of LTR-RE sequences in the genome was analyzed using RepeatMakser v4.1.1 (http://www.repeatmasker.org).

Library preparation of ALE-seq

Total DNA was extracted from samples using an improved CTAB method optimized for Moso bamboo (Gao et al., 2006) DNA fragments ranging from 4k to 15k bp were recovered from agarose gel after electrophoresis. The recovered DNA fragments were used to construct ALE-seq libraries following the previously described methods (Cho et al., 2018). Two active *Arabidopsis* LTR-REs, *Evade* and *Onsen*, were added to the extracted Moso bamboo DNA as internal controls (Matsunaga et al., 2011; Cho et al., 2018). Subsequently, the libraries were sequenced on MiSeq v3 2×300 bp

188 platforms. Sequences of the primers used in the construction of ALE-seq library are provided in
189 Table S1.
190
191 **Analysis of ALE-seq data**
192 Trimmomatic v0.39 (Bolger et al., 2014) was used to remove the adapters and low-quality
193 reads from the ALE-seq raw data. Reads were then mapped to the Moso bamboo genome using
194 Bowtie2 with default parameters (Langdon, 2015). The "MarkDuplicates" function of Picard
195 package (http://broadinstitute.github.io/picard/) was used to remove duplicate reads generated by
196 PCR amplification during the library preparation.
197 MACS v2.2.7.1 (Feng et al., 2012) and Bedops v2.4.39 (Neph et al., 2012) were used to
198 perform peak calling and merging the overlapping regions with default parameters, respectively.
199 The eclDNA abundance of LTR-REs was assessed using Bedtools with sub-function "multicov"
200 (Quinlan & Hall, 2010). Finally, the statistical significance test for eclDNA levels was carried out
201 using DESeq2 (Love et al., 2014). The LTR-REs with Log2FoldChange (FC) ≥ 2 and adjusted $P <$
202 0.05 were considered to be significantly up-regulated.
203
204 **RNA-seq library construction and RNA-seq analysis**
205 Total RNA was isolated from samples using the RNAprep Pure Plant Kit (product No. DP432,
206 TIANGEN, China) following the manufacturer's instructions. RNA-seq libraries were constructed
207 using the TruSeq RNA Sample Prep Kit (Illumina, CA, USA). The libraries were then sequenced
208 with the 150-nt paired-end mode on an Illumina HiSeq2500 platform at Biomarker Technologies
209 in Beijing, China (http://www.biomarker.com.cn).
210 After filtration of low-quality reads with Trimmomatic v0.39, clean reads were mapped to the
211 Moso bamboo genome and the curated LTR-RE, and the abundance was quantified using STAR
212 (https://github.com/alexdobin/STAR) (Varet et al., 2016). DESeq2 was used to assess the statistical
213 significance of the expression levels of LTR-REs and genes..Log2FC| ≥ 1 and adjusted P value <
214 0.05 were used to define differentially expressed LTR-REs and genes.
215
216 **Functional enrichment and Cis-element detection**
217 GO and KEGG enrichment analyses were performed using Gogsea and Pathwaygsea,
218 respectively, on Omicshare v4.1.0 platform (https://www.omicshare. com/tools/). PlantCARE
219 (Lescot et al., 2002) were using to identify cis-acting regulatory elements.
220
221 **WGBS of Moso bamboo seedlings under abiotic stresses**

WGBS data for Moso bamboo seedlings under abiotic stresses, including salt (Salt) and UV treatments, as well as control samples, were obtained from our previous work (Ding et al., 2022). The control samples included two types: the seedlings subjected to no stress served as the control group (CK) and seedlings irrigated with water (Wa) without NaCl served as the control for Salt. The stress treatment procedures and stages of plants were identical to those other samples in this study. We followed the analysis pipeline described in (Ding *et al.*, 2022) to perform data quality control and data analysis.

Identification of insertion sites of LTR-REs

The whole-genome bisulfite sequencing data were aligned to the Moso bamboo genome using Bismark v0.23 (Krueger & Andrews, 2011) and the unmapped reads were retrieved. These unmapped reads were used to identify insertion sites of LTR-REs with EpiTEome v1.0 (Daron & Slotkin, 2017) using the parameters set with "-l 150 -b 50000 -p 50".

Identification of new insertion sites of *PHRE11* and *PHRE12*

The insertion sites of *PHRE11* and *PHRE12* in Moso bamboo under stress conditions and during development were mapped by transposon display followed by Sanger sequencing. After RNA elimination, the genomic DNA was digested using the restriction endonuclease *Sau*3AI (Takara 1069A, Japan) and then ligated with a cassette adaptor using Hi-T4 DNA Ligase (Cat. M2622; New England Biolabs, USA). Subsequently, PCR amplifications were performed following the procedure of TaKaRa LA PCR™ *in vitro* Cloning Kit (TaKaRa RR015, Japan). The PCRs generated DNA fragments containing the LTR-RE end flanked with genomic DNA region. After polyacrylamide gel electrophoresis, polymorphic bands were isolated and DNA was recovered to analyzed by Sanger sequencing to confirm the new insertion sites of *PHRE11* and *PHRE12* in Moso bamboo. New insertion sites of *PHRE12* in transgenic Moso bamboo and *Arabidopsis thaliana* were identified using the procedure described above. The sequences of the adapter and primers are presented in Table S2.

Transgene validation of activated LTR-REs

The primers for *PHRE11* PCR amplification are listed in Table S3. *PHRE11* was recombined into the binary vector pCAMBIA3301 using the ClonExpress II One Step Cloning Kit (Vazyme C112; China). To detect the transposition events of *PHRE11* in the host genome, a *HygR* gene expression unit (CaMV 35S promoter::*HygR* gene::CaMV poly(A) signal) was inserted downstream of *pol* domain and upstream of 3'LTR. The construct was introduced into wild-type

Arabidopsis thaliana Col-0 with the floral dip method using *Agrobacterium tumefaciens* strain GV3101. The transgenic *Arabidopsis thaliana* plants from T1 to T3 generations were tested for hygromycin resistance and the presence of *HygR* by PCR amplification. The primers are presented in Table S4. The seedlings survived in the hygromycin-containing media were further tested for the copy number of *PHRE11* using qPCR method as described in Zhou et al. (Zhou et al., 2018). The primer sequences are listed in Table S5. New insertions of *PHRE11* were detected with a chromosome walking kit (Code No. 6108, TaKaRa Bio Inc., Japan). The specific primers from *HygR* used in the chromosome walking procedure were listed in Table S6.

The same construct was simultaneously introduced into Moso bamboo calli using carbon nanotube-mediated DNA delivery (Demirer et al., 2019). Calli were soaked in the DNA delivery buffer with both PEI-SWNTs and the recombinant vector for two days. After surface cleaning, the infected calli were sub-cultured on the MS medium containing hygromycin for selection. New tissues germinated from surviving calli were tested for the presence and expression of *HygR* gene by PCR amplification and reverse transcription (RT-) PCR, respectively. The primer sequences are listed in Table S5. New insertions of *PHRE11* were also detected using the method described above.

Quantitative PCR (qPCR)

The levels of eclDNA of LTR-REs were measured by qPCR using the ALE-seq library DNA as templates. *Onsen* and *Evade* DNA were used as reference DNA in the qPCR analyses. RNA levels of LTR-REs were determined by qPCR amplifying the 5'LTR sequences. *Actin8* was used for normalization.

The copy number of *PHRE11* in transgenic plants was calculated by absolute quantification of RNA-free genomic DNA. *AtACTIN8* was used as a reference gene and to formulate the standard curve for quantification. The formula of the standard curve is $y = -3.5245x + 37.744$ ($R^2 = 0.995$). The exogenous *HygR* gene integrated into *PHRE12* was used to quantify the copy number of *PHRE11*.

These qPCR reactions were conducted with Hieff® qPCR SYBR Green Master Mix (No Rox; YESAN, Shanghai, China). The primer sequences used in the qPCR experiments are listed in Supplemental Table 5, 7 and 8.

Results

Identification of active Moso bamboo LTR-REs

In order to profile the active LTR-REs, the Moso bamboo genome sequences (Zhao *et al.*, 2018) was first re-investigated to curate a comprehensive set of transposons. Using the LTRpred and LTRdigest pipelines, we identified a total of 1,014,565 LTR-REs, including 7,731 full-length intact elements. The proportion of LTR-RE sequences was 54.97% of the genome by length (Table 1). Careful inspection of their sequences found that Ty1-*Copia* and Ty3-*Gypsy* superfamilies had diverse usage of PBS motifs (Table S9). MetCAT24 and LysTTT were the most common PBS motifs associated with 83.42% of LTR-REs in Moso bamboo, therefore, these sequences were chosen to enrich LTR-REs in the ALE-seq experiments that will be detailed below.

Table 1. Classification of LTR-REs in Moso bamboo genome.

Superfamily	Lineage	Family[a]	Structure	Number[b]	Ratio (%)	Length (bp)	Content (%)
Ty1-*Copia*	*tork*	236	GAG-PR-INT-RT-RH	145708	14.36	124219995	6.51
	retrofit	342	GAG-PR-INT-RT-RH	41965	4.14	43615815	2.29
	sire	136	GAG-PR-INT-RT-RH-ENV	223386	22.02	210097734	11.01
	oryco	105	GAG-PR-INT-RT-RH	22078	2.18	22854591	1.20
	Total	819		433137	42.69	400788135	21.01
Ty3-*Gypsy*	*del*	207	GAG-PR-RT-RH-INT-CHR	295222	29.10	334005916	17.51
	reina	249	GAG-PR-RT-RH-INT-CHR	27803	2.74	39235939	2.06
	crm	47	GAG-PR-RT-RH-INT	40781	4.02	44298955	2.32
	tat	238	GAG-PR-RT-RH-INT	217288	2.14	230055053	12.06
	Total	743		581428	57.31	647905081	33.96
Total		1562		1014565		1048693216	54.97

[a] represents the family number in individual lineage.

[b] represents the number of LTR-REs in Moso bamboo genome.

[c] represents the proportion of each lineage in Moso bamboo genome.

To identify active Moso bamboo LTR-REs that are potentially mobile, we collected samples from the stressed seedlings (Heat, Cold, UV, and Salt] and at various developmental states of shoot tissues (ICD, RCD, RCE, GSI, and YSI), meristematic tissue (Calli), and intercalary meristems in shrunk (IMS15) and lengthened (IML15) parts of 15th twisted internodes (Fig. 1). Using these samples, we carried out ALE-seq and RNA-seq experiments to measure the levels of DNA and RNA intermediates, which will collectively be used to identify active LTR-REs. After cleaning and mapping of sequenced reads, the reproducibility of the ALE-seq samples was examined by

clustering analysis based on Euclidean distance. Fig. S1 shows moderate to strong reproducibility among the samples in different stress treatments and developmental stages. DESeq2 analysis identified a varying number of significantly up-regulated eclDNAs, ranging from 0 to 3,676 in 11 different comparisons (Table 2). A relatively higher number of up-regulated eclDNAs were observed in the samples treated with UV (n=3,676), Salt (n=3,166), ICD (n=2,669), and Calli (n=2,646), while other samples possessed far fewer up-regulated eclDNAs (Table 2). In addition, 2,239 LTR-REs were commonly found to be up-regulated in eclDNA levels in the four types of samples (Fig. 2a).

Table 2. Number of LTR-REs with significantly increased abundance of eclDNA and (or) RNA in each comparison.

Sample	Elongation internodes		Color variation internodes		Form variation internodes		Seedlings under abiotic stress					Union
	RCE	ICD	YSI	GSI	IMS15	IML15	Heat	Cold	UV	Salt	Calli	
eclDNA	21	2 669	15	101	0	25	25	31	3 676	3 166	2 646	4 201
RNA	236	3 938	235	289	25	60	119	27	3 638	3 726	3 966	5 438

RNA-seq was also carried out using the samples as above and were analyzed to quantify the RNA levels of LTR-REs. Consistent with the ALE-seq data, a greater number of significantly up-regulated LTR-REs were found in Calli (n=3,966), ICD (n=3,938), Salt (n=3,726) and UV (n=3,638) samples, and much smaller number of up-regulated LTR-REs were found in other samples (Table 2). Amongst those with increased RNA levels, 3,607 of them were commonly appeared as up-regulated by the treatments (Fig. 2b).

A total of 2,170 LTR-REs, accounting for 0.21% of all LTR-REs, were significantly and commonly up-regulated in both ALE-seq and RNA-seq (Fig. 2c; hereinafter defined as 'active' LTR-REs). Detailed information of these 2,170 is curated in Table S10. The proportions of the Ty1-*Copia*, Ty3-*Gypsy* and other superfamilies in these active LTR-REs were 56%, 39% and 5%, respectively (Fig. 2D). The largest number of LTR-RE was detected in *tat* lineage (24%), followed by *reina* (21%) and *tork* (14%) successively (Fig. 2d), which differ from the genomic copies composition (Table 1), indicating a stress- and developmental stage-specific activation of LTR-REs.

The top twenty-two most significantly up-regulated elements in the ALE-seq data (Log2FC ≥ 10 and *FDR* < 0.00001; Table S11) among the 2,170 LTR-REs were selected for further qPCR validation detecting eclDNA and RNA levels. The qPCR results showed that these LTR-REs

exhibited significantly up-regulated levels of both eclDNA and RNA in the stressed samples compared to the control samples (Fig. S2 and S3).

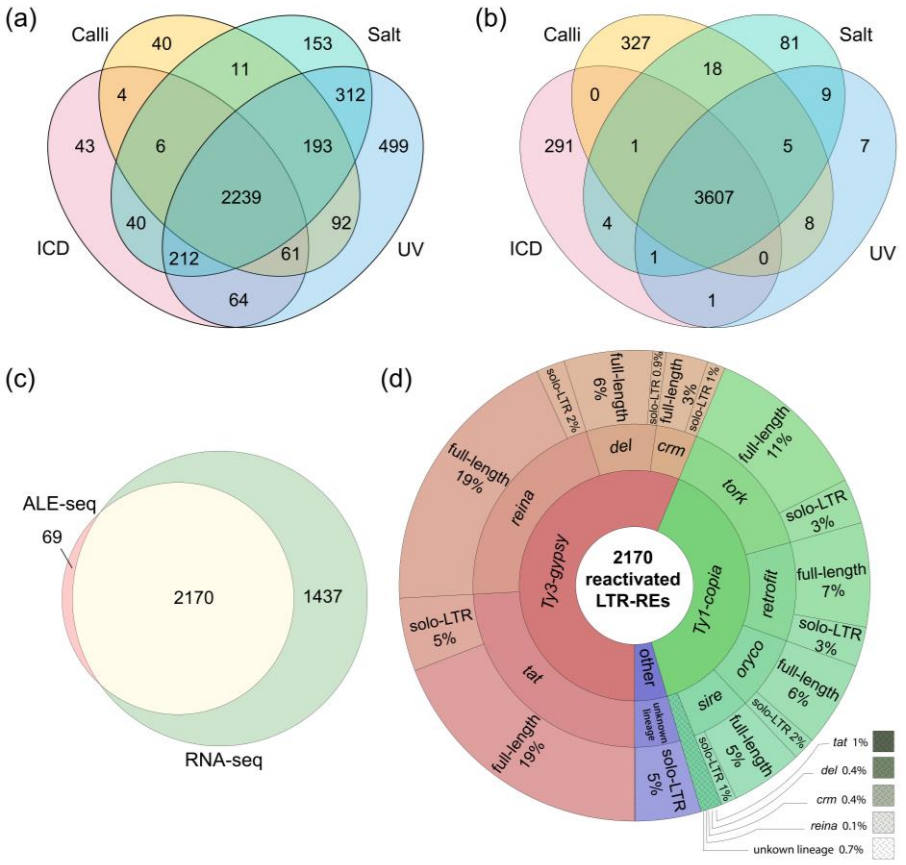

Fig. 2. Venn diagram of LTR-REs with significantly up-regulated abundance in treatments, different development stages and variation tissues. (a) LTR-REs with significantly up-regulated eclDNA abundance in ALE-seq. (b) LTR-REs with significantly up-regulated expression in RNA-seq. (c) LTR-REs with up-regulated abundance in both ALE-seq and RNA-seq. (d) Classification of the 2,170 LTR-REs.

Genomic and epigenomic features of active LTR-REs

The active LTR-REs were unevenly distributed across the chromosomes, whilst the four samples (ICD, Calli, Salt, and UV) exhibited a largely similar pattern of their chromosomal locations (Fig. 3a). Of note, the active LTR-REs were strongly associated with the gene-rich regions, and in fact, 97.73% of these retroelements are located within 2,000 bp from the closest genes (Fig. 3b). In addtion, the LTR regions of these active LTR-REs contain cis-regulatory elements including those involved in the hormonal singalling (auxin and gibbereillin), stress response, cell cycle regulation, meristematic growth and core promoter elements (Fig. 3A and Table

S12). Hence, these collectively suggest that the active LTR-REs might be functionally associated with the neighbouring genes in the control of stress tolerance and development.

To further investigate the functional relevance of active retroelements on the neighboring genes, we retrieved the sequences of 2,014 genes that are within 2,000 bp from the active LTR-REs and assessed their treanscript levels. Intriguingly, many of these genes were strongly up-regulated in the Salt and UV samples (Fig. 3c). Additionally, the gene ontology analyses identified the genes in the hyperosmotic salinity response, 6-phosphofructo-2-kinase activity, arginine catabolic process to proline, DNA metabolic process, DNA repair complex, cell cycle checkpoint and chromosome were enriched (Fig. S4). KEGG analysis showed that the pathways in the ubiquinone and other terpenoid-quinone biosynthesis, alpha-linolenic acid metabolism, glycan degradation, peroxisome, autophagy and oocyte meiosis were significantly enriched (Table S13). This is in line with the fact that DNA metabolic process and DNA repair complex are associated with UV stress; hyperosmotic salinity response, 6-phosphofructo-2-kinase activity, and arginine catabolic process to proline with NaCl stress; and cell cycle checkpoint and chromosome with cell growth factors act in the plant development and growth.

We next wanted to understand how the active LTR-REs are induced in specific conditions. Since the DNA methylation can be drastically altered in response to stresses and critical developmental transition, we examined the epigenome changes induced by the treatments using the whole-genome bisulfite sequencing (WGBS) dataset generated in our previous study (Ding et al., 2022). Although the plant samples [UV, CK (control to UV), Salt and Wa (irrigation with water; control to Salt)] were prepared independently, they were grown and treated with stresses in the same way as those plants used for RNA-seq and ALE-seq. Importantly, the DNA methylation profiling in the 2,170 ative LTR-REs showed that the UV and Salt samples exhibited reduced DNA methylation compared to the CK and Wa in all cytosine contexts (Fig. 3d). These results support the notion that the increased expression of the active retrotransposons might be attributed to the reduction of DNA methylation, and partly account for the induction of the neighbouring genes as well. These altogether might indicate that the active LTR-REs, together with the associated genes, constitute specific gene regulatory networks through both genetic and epigenetic signals, potentially benefiting the host plants with stress response and growth regulation.

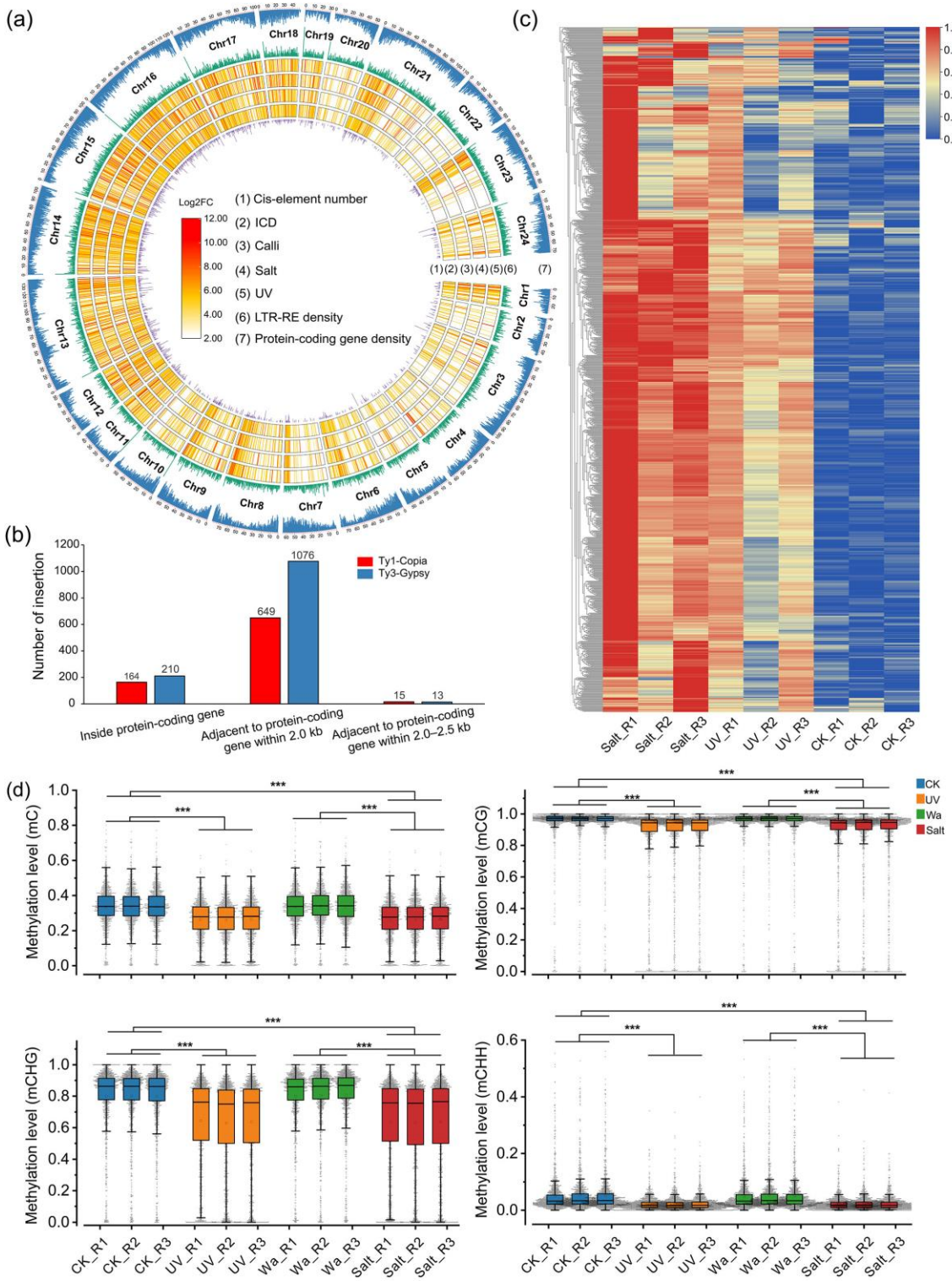

Fig. 3. Distribution, expression and methylation of the 2,170 activated LTR-REs. (a) Circos plot shows the distribution of LTR-REs and protein-coding genes on genomic chromosomes. The average Log2Foldchages of the activated LTR-REs in ICD, Calli, Salt, and UV were also presented. (b) Histogram of the number of LTR-REs related to coding genes regions. (c) Expression profile of the genes adjacent to the 2,170 activated LTR-REs in Salt, UV and CK samples. (d) Methylation profile of the activated LTR-REs in CK, UV, Wa and Salt samples, which contain three biological repeats, have been statistically analyzed. Wa, water-irrigated treatment, is another control for the salt treatment. Data is exclusively presented for LTR-REs with methylation profiles in all samples.

LTR-RE integration and epigenomic changes

To further investigate the functional impact of the activated LTR-REs under stresses, the WGBS data were used to synchronously detect new insertion sites and their DNA methylation levels in the Moso bamboo genome using the EpiTEome software (Daron & Slotkin, 2017). We identified 1,121 new insertions, 637 and 484 of which were detected in the UV and Salt samples, respectively, and were contributed by similar classes of transposons (Fig. 4a). Remarkably, 922 of these new insertions were generated by the active LTR-REs (Fig. 4b), which further supports the robustness of the combined analysis of ALE-seq and RNA-seq of this study. Our alluvial map analysis found that a significant proportion of the new insertions was observed in Chr13, Chr14 and Chr12, successively (Fig. 4b). Of the 1,121 new insertions, 231 and 549 were found to be inserted into or near (< 2,000 bp) protein-coding genes, respectively (Fig. 4c). These data indicate that the active LTR-REs of Moso bamboo preferably insert to proximal intergenic regions near protein-coding genes. Furthermore, we found that the coding genes located within 5,000 bp of the new insertion sites of LTR-REs primarily act in the stress response, auxin transport, and high light intensity response (Fig. S5).

It is well documented that transposon insertions trigger DNA methylation changes around the inserted sities. To see if this can happen in the Moso bamboo genome, we examined DNA methylation levels around the regions where the active LTR-REs inserted. The flank sequences (< 1,000 bp) of new LTR-RE insertion sites (Neo-inserted) display lower DNA methylation levels than those of loci without new insertions (No-inserted) under the same treatment (Fig. 5). In particular, these hypomethylated regions of the adjacent coding genes may serve as transcriptional regulatory sequences, such as promoters and enhancers. Therefore, these results imply that the reduced DNA methylation levels might release transcriptional repression of the associated genes close to the active LTR-REs under stress, such as UV radiation and salt stress.

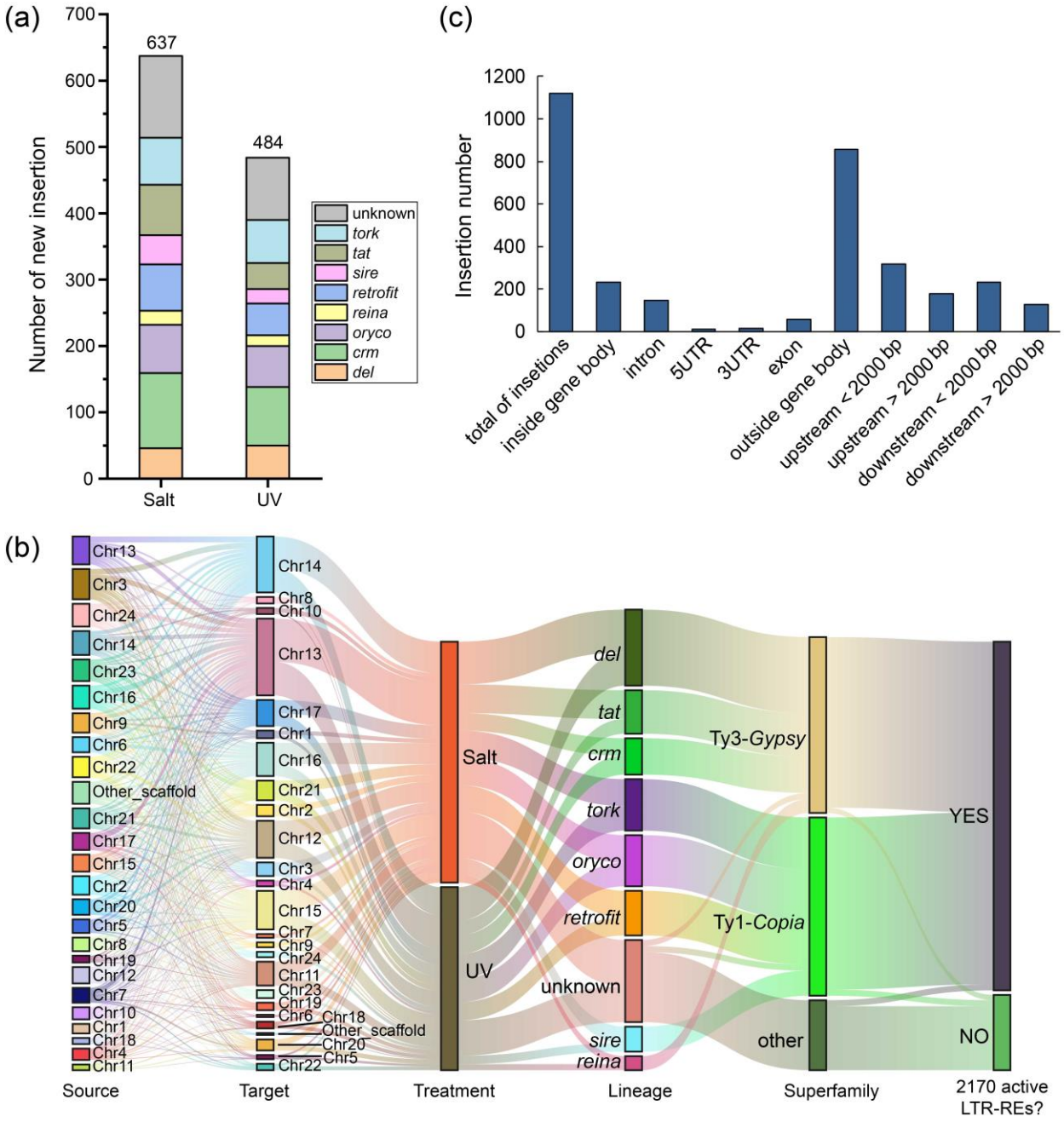

Fig. 4. New LTR-RE insertion characteristics based on WGBS data in UV and Salt treatments. (a) Proportion of lineage classification for the mobilized LTR-REs with insertions after Salt and UV treatment. (b) Alluvial plot shows classification features of LTR-REs with new insertion sites. (c) The positions of new insertion relative to neighbouring protein-coding genes.

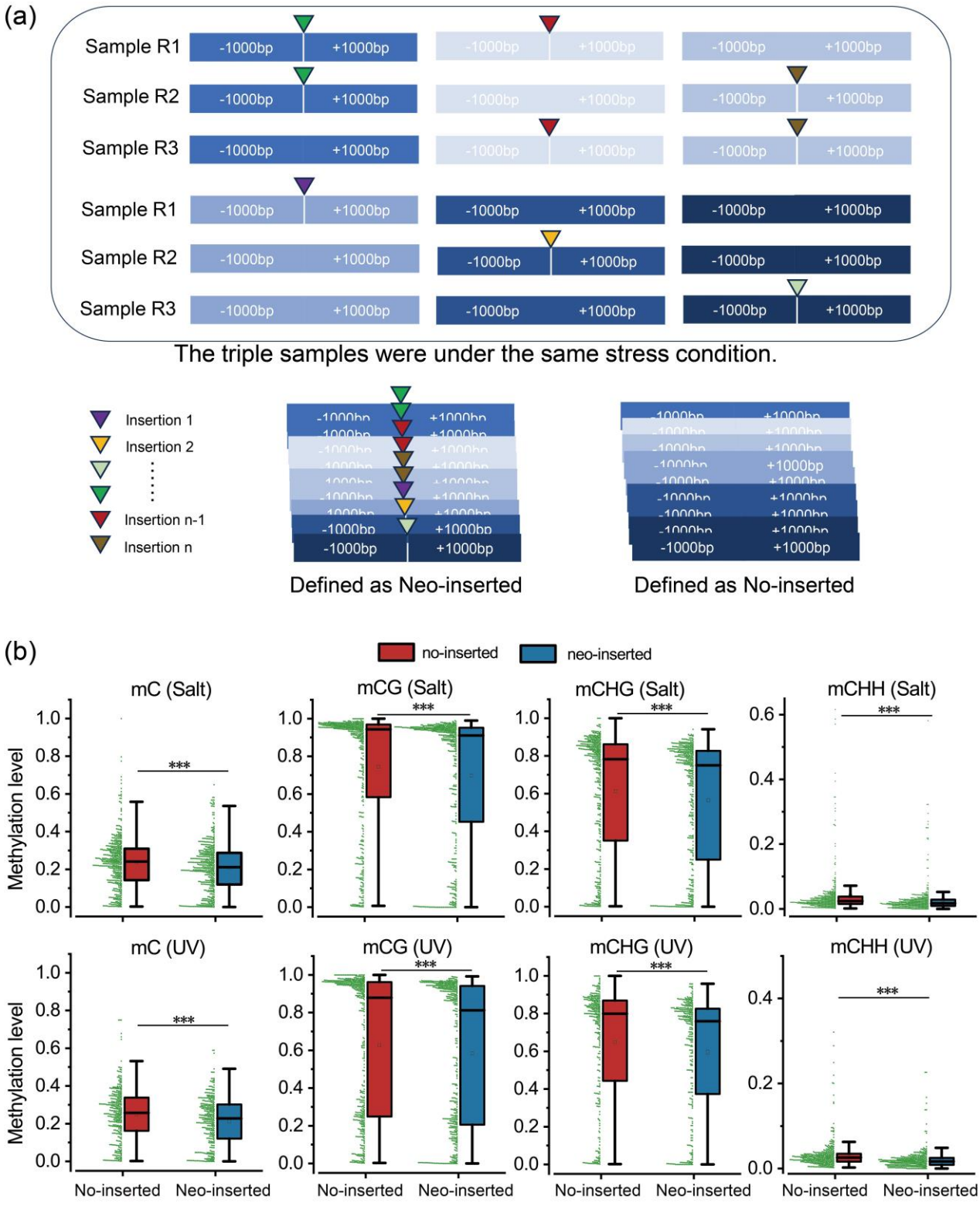

Fig. 5. Methylation levels of the new LTR-RE insertions based on WGBS data in UV and Salt treatments.

(a) Definition of both neo-insertion and no-insertion in the datasets generated from the same treatments. (b) Comparison of the methylation levels between the same sequence regions (1000 bp upstream and downstream) with new LTR-RE insertions and without new insertions during stress treatments.

Mobility of the active Moso bamboo LTR-REs

We then wanted to assess the transpositional activity of the active LTR-REs identified in this study, and to do this, the top twenty-two most significantly up-regulated LTR-REs (summarized in Table S11) were carefully examined for their protein domains and LTR sequences. Two LTR-REs were found to be complete and intact, containing the conserved *gag* and *pol* domains and high similarity between 5' and 3' LTR sequences. These two full-length LTR-REs from *Gypsy* superfamily were named *PHRE11* (*Phyllostachys edulis retrotransposon 11*) and *PHRE12* (*Gpysy* ; Table S11 and Fig. S6), and were further investigated for their new insertions in Moso bamboo seedlings subjected to abiotic stress and in Moso bamboo internodes.

To assess the transpositional activity of *PHRE11* and *PHRE12*, the transposon display technique was employed. As shown in Fig. 6, the polymorphic bands were observed for *PHRE11* in all of the samples tested and those for *PHRE12* in most of the samples except for GSI. The polymorphic bands were recovered from the gels for sequencing and determined for new insertion sites. Seven bands were identified as new insertions located within 1,500 bp upstream or downstream of protein-coding genes (Fig. 6). The analysis of sequence similarity has revealed the putative functions of these genes in response to stress or development. Specifically, the homologous genes of PH02Gene11330 (*GT-1*) and PH02Gene20741 (*PGR3*) from UV samples are associated with the light signaling (Ayadi et al., 2004) and photosynthesis (Yamazaki et al., 2004), respectively, while PH02Gene46833 (*CIPK23*) from Salt samples is involved in osmotic stress (GO:0006970). Additionally, PH02Gene28894 (*CSLD3*) from the ICD and PH02Gene36141 (*SAG12*) from calli play roles in vascular development (GO:0009833) and cell apoptosis (GO:0010623), respectively. Our analysis confirms that the active LTR-REs *PHRE11* and *PHRE12* are capable of inserting into new genomic positions under stress or during development. Moreover, our data indicates that the mobilization of transposons driven by stress may reconfigure the gene regulatory network by inserting close to key relevant genes.

(a)

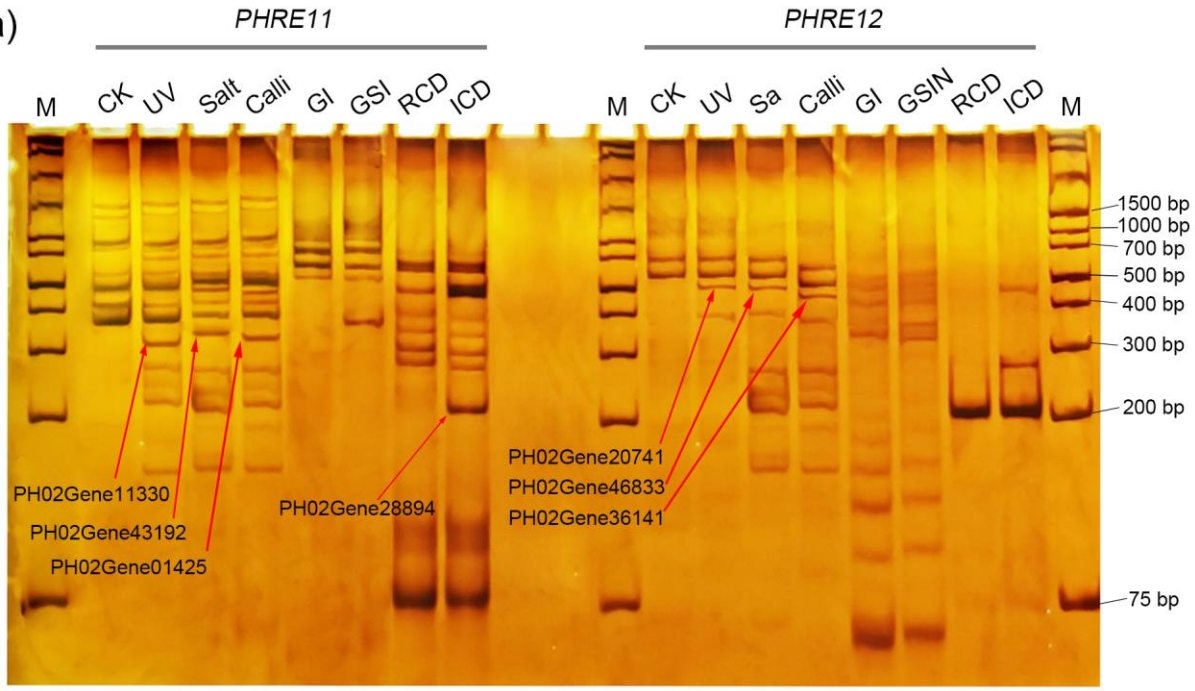

(b)

LTR-RE	Sample	Gene	BLAST position	Distance	Gene annotation
PHRE11	UV	PH02Gene11330	Chr23:30255407–30255617	1410 bp	transcription factor GT-4-like
	Salt	PH02Gene43192	Chr7:2318738–2318958	1420 bp	1molybdate transporter 1-like
	Calli	PH02Gene01425	Chr7:45894275–45894375	1300 bp	transcription factor RAX1-like
	ICD	PH02Gene28894	Chr13:120536485–120536585	1300 bp	cellulose synthase-1-like protein
PHRE12	UV	PH02Gene20741	Chr2:38133938–38131588	-1150 bp	pentatricopeptide repeat-containing protein
	Salt	PH02Gene46833	Chr13:1124657–1124387	930 bp	CBL-interacting protein kinase
	Calli	PH02Gene36141	Chr3:2079562–2079162	800 bp	ervatamin-B

Fig. 6. Detection of *PHRE11*'s and *PHRE12*'s new insertions using transposon display technique. (A) Polyacrylamide gel electrophoresis of polymorphism bands for detecting new LTR-RE insertions. M, DNA marker. The red arrows emphasized new insertions adjacent to protein-coding genes. (B) Protein-coding genes adjacent to *PHRE11*'s and *PHRE12*'s new insertion sites. Positive distance values indicate that the new LTR-RE insertions were discovered upstream of coding genes, while negative values indicate that they were found downstream of coding genes.

To further determine the mobilization characteristics of LTR-REs identified in this study, *PHRE11* was selected and introduced into *Arabidopsis thaliana*. *PHRE11*, tagged with the *HygR* gene between the *pol* domain and 3' LTR region, was cloned downstream of 35S promoter of pCAMBIA3301 vector (named pCAMBIA3301-*PHRE11*; Fig. 7a). The transgenic *Arabidopsis* plants were confirmed by the presence of the *HygR* gene (Fig. S7), and four independent transgenic lines were obtained (Table 3; T1-1 to T1-4). We used qPCR to measure the copy number of *PHRE11* in the genomic DNA of the descendants of *A. thaliana* transgenic lines. A greater number

of *PHRE11* copies were detected as generation progressed, indicating that *PHRE11* transposed during inbreeding of the transgenic plants. This pattern was most prominently observed in the T2-2-2 offsprings (T3 generation: T3-2-2-2 and T3-2-2-3; Table 3). In line with this observation, the T2-2-x lines (T2-2-1, T2-2-2, T2-2-3 and T2-2-4; Table 3) and T2-2-2's offsprings exhibited vegetative growth defects with distinct reduction in leaf area, number, and stature than the wild-types (Fig. 7b, c). We further carried out chromosome walking experiments to identify the new insertions of *PHRE11* in T3-2-2-2 and T3-2-2-3, and two insertions were identified in AT4G17140 and AT2G19690 (Table S14). These data further provide *ex situ* evidence that *PHRE11* is able to transpose and partly suggest its insertion perference towards protein-coding genes.

The vector pCAMBIA3301-*PHRE11* was also introduced to moso bamboo by co-cultivating the plasmid with the calli in the PEI-SWNTs (Polyethylenimine Functionalized Single-Walled Carbon Nanotubes) DNA delivery buffer (Fig. 7a, d). After the sub-culture in the hygromycin media, the newly grown calli were tested for *PHRE11* transposition. The *HygR* gene integrated into *PHRE11* was successfully amplified from the fresh calli by PCR (Fig. 7e), and the RT-PCR experiments revealed that *HygR* is expressed in the newly proliferated calli (Fig. S8). Furthermore, chromosome walking was performed to map the new insertions in the transformed calli (Fig. 7f). These insertion sites were located in Chr3, Chr17 and Chr21, respectively (Table S15). These results together indicate that *PHRE11* is mobile in the Moso bamboo.

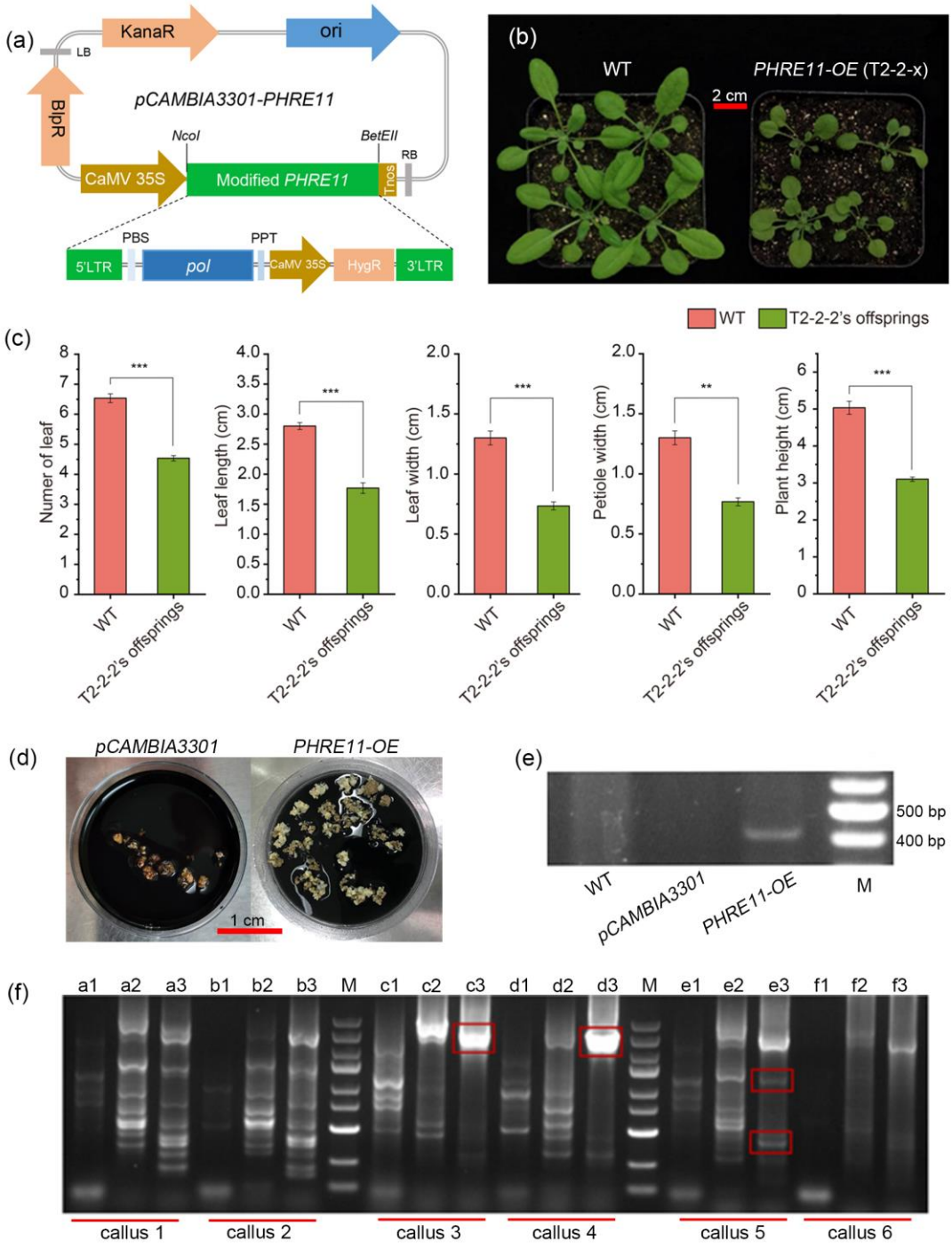

Fig. 7. *PHRE11* transgene into *Arabidopsis thaliana* and Moso bamboo calli. (a) *pCAMBIA3301-PHRE11* vector construction. (b) wild-type and *PHRE11-OE* (T2-2-2) *A. thaliana* plants, showing the vegetative phenotypes. (c) Statistics of plant vegetative traits for wild-type and *PHRE11-OE* plants. $^{**}P < 0.01$ and $^{***}P < 0.001$, by Tukey test. (d) Transgene scene of *pCAMBIA3301-PHRE11* into Moso bamboo calli. (e) *HygR* were onlyamplified from the transgenic calli by PCR. (f) Chromsome walking experiment for detecting the transposition of the modified PHRE11 in subcultured calluses. Primary PCR: lanes a1, b1, c1, d1, e1, and f1; Secondry PCR: lanes a2, b2, c2, d2, e2, and f2; Tertiary PCR: lanes a3, b3, c3, d3, e3, and f3. Only those plain products from tertiary PCR were used to detecte transpositions of the modified *PHRE11*. The PCR products of PHRE11, surrounded by the red box in the electrophoretogram, were found to be inserted near coding genes. M, DL 5000 bp DNA Marker; WT, wild-type.

Table 3. *HygR* copy number in transgenic *A. thaliana.*

T1	copy number	T2	copy number	T3	copy number
T1-1	2.63	T2-1-1	2.90	T3-1-1-1	3.02
				T3-1-1-2	5.61
				T3-1-1-3	1.51
		T2-1-2	5.35	T3-1-2-1	4.84
				T3-1-2-2	9.75
				T3-1-2-3	4.98
		T2-1-3	9.16	T3-1-3-1	5.75
				T3-1-3-2	2.20
				T3-1-3-3	2.93
T1-2	13.14	T2-2-1	19.69	T3-2-1-1	10.47
				T3-2-1-2	20.44
				T3-2-1-3	31.93
		T2-2-2*	7.08*	T3-2-2-1*	7.80*
				T3-2-2-2*	10.62*
				T3-2-2-3*	11.48*
		T2-2-3	12.30	T3-2-3-1	21.80
				T3-2-3-2	17.25
				T3-2-3-3	3.67
		T2-2-4	20.61	T3-2-4-1	20.24
				T3-2-4-2	18.66
				T3-2-4-3	22.87
T1-3	3.41	T2-3-1	2.17	T3-3-1-1	2.07
				T3-3-1-2	2.36
				T3-3-1-3	2.40
		T2-3-2	6.14	T3-3-2-1	2.63
				T3-3-2-2	4.47
				T3-3-2-3	4.77
		T2-3-3	2.29	T3-3-3-1	2.20
				T3-3-3-2	1.70
				T3-3-3-3	1.95
T1-4	3.90	T2-4-1	1.43	T3-4-1-1	4.76
				T3-4-1-2	1.12
				T3-4-1-3	4.17
		T2-4-2	2.53	T3-4-2-1	2.24
				T3-4-2-2	1.23
				T3-4-2-3	3.51
		T2-4-3	3.33	T3-4-3-1	2.27
				T3-4-3-2	2.38
				T3-4-3-3	5.35

* highlights T2-2-2 and its descendants

Discussion

LTR-REs have successfully proliferated in the genomes of higher plants, resulting in a significant increase in genome size and creating genetic variability (Lisch, 2012). Historical transposition events caused diverse changes in the structure and expression of genes (Hirsch & Springer, 2017). Although LTR-REs are abundant in plant genomes, majority of them are normally quiescent in transposition (Schorn et al., 2017). Nonetheless, many studies demonstrated that retrotransposons can be activated by stress and developmental signals of the host genome. Mobilization of retrotransposons plays important roles in the stress resistance (Waititu et al., 2020), metabolic process (Butelli et al., 2012), and development, through either *cis* or *trans* regulation and/or spreading of DNA methylation (Gutzat *et al.*, 2020; Canat & Torres-Padilla, 2021). Unfortunately, studies so far only inspected single or a few LTR-REs for their roles in plant gene regulation. The comprehensive examination of large-scale transposons involved in the regulation of gene transcription in response to abiotic stress and development remains deficient, greatly limiting our ability to grasp the inherent significance of the temporally activated LTR-REs. Therefore, we utilized various techniques to investigate transpositionally and transcriptionally competent LTR-REs and their impacts on the gene control in Moso bamboo.

LTR-REs can be activated by environmental stimuli or the developmental state of their host cells, but their responses to various stresses and developmental phases are markedly heterogeneous. We tested multiple stresses and developmental stages of Moso bamboo and identified thousands of active LTR-REs in this study (Fig. 2 and Table 2). The active LTR-REs exhibited some degree of variability across different stresses and developmental tissues, but a substantial number of them were found active commonly in Calli, ICD, Salt, and UV samples, and it was marginal in other samples under specific conditions. Fan et al. (2013) found that *Pinus massoniana* needles showed few activation of LTR-REs in response to extreme temperatures like heat and cold. However, they observed a genome-wide transcriptional activation of LTR-REs when the needles were exposed to UV light and various phytohormone treatments. The LTR-REs in pitaya (*Hylocereus undatus*) are strongly activated under cold and salt stress, with a relatively weaker response to heat stress and UV exposure (Nie et al., 2019). In Arabidopsis, the shoot apical meristem cells in the early stages of vegetative growth demonstrate elevated transposon activity (Gutzat et al., 2020). Collectively, these suggest that the extent of transposon activation is subject to fluctuations based on the prevailing stress and developmental circumstances, as well as the particular species under consideration.

In general, DNA methylation levels remain relatively constant across plant tissues, except for the juvenile and fast-growing stages (Bartels et al., 2018). This is consistent with the previous

studies suggesting that global methylome changes were only marginal (Korotko et al., 2021; Ding et al., 2022). Given these observations, the reduced activation of LTR-REs detected in the samples (GSI, IML15, IMS15, RCE, YSI, and heat/cold stress leaves; Table 2) might be due to the limited DNA methylation changes or the inhibition from hypermethylation. Ding et al. (2022) observed that both cold and heat stress induce the excessive elevation of hyper CHG methylation in Moso bamboo genome, which in turn restrains transposon activity (Wang et al., 2018). Conversely, the samples that underwent UV radiation and salt stress were found hypomethylated in CHG (Ding et al., 2022). Then, they manifested an exceedingly high copy number of active retrotransposons (Fig. 2 and Table 2). It was known that UV radiation and salt stress can potentiate global DNA demethylation in plant genomes (Jiang et al., 2021; Skorupa et al., 2021). In our methylome data, most of LTR regions of the active LTR-REs in the UV and Salt samples showed reduced DNA methylation levels (Fig. 3D), which can account for the high number of reactivated retrotransposons by the two stress treatments. More recently, Ding et al. (2024) also found that hypomethylation of LTR regions accounts for LTR-RE activation during abiotic stress. Additionally, previous studies demonstrated that DNA methylation is drastically lost during callus culture (Gao et al., 2014), which then results in transpositional burst of transposable elements (Hu et al., 2019). Consistently, we found 3,966 reactivated LTR-REs in the tissue cultured samples (Table 2). Moreover, it is well documented that transposable elements are globally methylated in plant meristems to maintain genome stability (Baubec et al., 2014). However, a more recent study demonstrated that transposable elements become activated in the shoot apical meristems at an early vegetative phase (Gutzat et al., 2020). In agreement with this notion, we identified high number of reactivated LTR-REs in Moso bamboo at ICD but low number at RCE (Table 2).

LTR-REs are more frequently found in the pericentromeric regions of plant genomes (Paterson et al., 2009; Wei et al., 2013). Some LTR-REs prefer to insert into gene coding regions, however, they can be subjected to purifying selection to avoid adverse effects of gene disruption (Wright et al., 2003; Paterson et al., 2009). Although the overall distribution of LTR-REs is inversely correlated with that of coding genes in Moso bamboo (Zhou et al., 2017b), the reactivated LTR-REs in the current study show distinctive distribution bias on chromosomes (Fig. 3a). Notably, these elements were frequently observed in the vicinity of protein-coding genes, within a range of 2,000 bp, and a small proportion of them were located within gene bodies (Fig. 3b). Intriguingly, the new insertions derived from LTR-REs reactivated by UV and Salt also exhibit a propensity to integrate into the vicinity of the coding genes (Fig. 4c). The insertional preference to genes has been well documented for heat-stressed activated *Onsen*, which approximately 81% of its insertion events occurred inside gene bodies (Gaubert et al., 2017).

Since eclDNA is the final intermediate of the retrotransposition process (Griffiths et al., 2018; Cho et al., 2018), we performed further experiments to verify the integrational activity of these reactivated LTR-REs, such as *PHRE11* and *PHRE12* (Fig. 6a). All the new insertion sites were located near the protein-coding genes with distances less than 1,500 bp (Fig. 6b), which is similar to what was observed for the genomic distributions of the active retrotransposons and their new insertions induced by stress conditions (Fig. 3b and Fig. 4c). Interestingly, all the genes associated with the new insertions of both *PHRE11* and *PHRE12* share common functional linkages to the given treatments and development (Fig. 6). For example, *PHRE11* in ICD inserted close to PH02Gene28894 (*CSLD3*), which is involved in the synthesis of polymers for the fast-growing primary cell wall (Wang et al., 2001). Considering that the transposition event is highly dynamic and shows heterogeneity in different tissues and even at single cell levels, we demonstrate that LTR-REs might have inserted close to the relevant genes under specific conditions to meet developmental demand or adapt to changing environment. It is possible that the tendency of these LTR-RE insertions near (or in) stress- and development-related genes might be due to the increased expression of the genes, which may create opportunities for chromatin opening, or be caused by other unknown molecular mechanisms. However, these questions still require further investigation of transpositional dynamics in different cells upon various environmental factors.

In our study simultaneously detecting the new insertions of LTR-REs and the DNA methylation of the flanking regions of these insertion sites, the insertion of LTR-REs at new sites will generally result in a significant decrease in the methylation level of adjacent sequences (< 1,000 bp) when compared to the absence of LTR-REs insertion under the same stress conditions (Fig. 5b). More recently, Noshay *et al.* (2019) suggested that transponson insertions can induce higher DNA methylation around the insertion regions in maize. In fact, opposing observations were previously made in different studies that transposon insertions can either increase or decrease the DNA methylation levels in the flanking DNA (Drongitis et al., 2016; Choi & Purugganan, 2017), such divergence of which might be determined by certain genetic context (Noshay et al., 2019). In short, our results suggest that LTR-REs insertions can change the methylation pattern in the regions around new insertions under specific conditions.

The transposon's LTR regions have the capacity to function as promoters and/or enhancers, thereby governing the expression of neighboring genes (Grandbastien, 2015; Canat & Torres-Padilla, 2021). The LTR sequences of the active LTR-REs in this study are enriched with cis-elements associated with stress responsiveness, auxin and gibberellin response, and cell growth (Fig. 2a and Table S12). Therefore, we reasoned that the active LTR-REs might involed in the expression of the nearby genes, which are enriched in some relevant functions or pathways involved

in stress responses and cell growth (Fig. S4; Table S13), through cis-acting. This hypothesis was supported by the synchronously increased expression of genes near the activated LTR-REs under the same conditions (Fig. 3c). Similar results were found in the work of Makarevitch *et al.* (2015) which revealed that many transposons can serve as promoters or enhancers to stimulate the expression of nearby stress-responsive gene under abiotic stress in maize. In addition, our transgenic approaches of *Arabidopsis thaliana ex situ* and Moso bamboo *in situ* experiments have demonstrated that the insertion of active *PHRE11* is feasible either within or in close proximity to genes (Fig. 7, Tables S14 and S15). Interestingly, the offsprings of transgenic line T2-2-2 with a high copy number of *PHRE11* exhibited vegetative growth defects showing reduced plants size compared to the wild type (Table 3; Fig. 7b, c). We identified two insertion sites of *PHRE11* in these dwarfish plants and one of the insertion sites was inside AT2G19690, a gene involved in growth and development (Lee et al., 2003), and the other insertion in the upstream of AT4G17140, a pleckstrin homology gene. Thus, the dwarfism of the transgenic lines might be resulted from the malfunction of the two genes. Altogether, these data provide appropriate examples that mobilization of LTR-REs reshapes the gene regulatory network in stress response and development in Moso bamboo.

In this study, we systematically captured a large mount of active LTR-REs induced by mutiple stress conditions and specific developmental stages using an integrated approach coupling ALE-seq and RNA-seq. We found that most of the reactivated retroelements are strongly correlated geographically and transcriptionally with protein-coding genes involved in stress resistance and development. The regions flanking the new inserted active LTR retrotransposons show reduced methylation levels under stress conditions, suggesting their role in regulating the expression of neighboring genes. The genic perference of transposition for LTR-REs and their impact on the expression of stress-responsive and development-related genes were validated with representative transposons. Our results address the potential adaptive role of LTR-RE-mediated remodulation of gene expression involved in stress response and development. These efforts lay the foundation for further research on the mechanism of LTR-REs in regulating plant growth and development.

Acknowledgments

This work was supported by the Zhejiang Provincial Natural Science Foundation of China (Grant No. LZ24C160002) and the National Natural Science Foundation of China (Grant No. 31870656). We thank Ms. Ya-Qian Yang and Dr. Guiyun Tao for Sample collections.

Competing interests

The authors declare no competing interests.

Author contributions

L.H.Z. performed experiments, analyzed data, prepared figures, and wrote the manuscript draft. B.Z. analyzed the the WGBS data, prepared figures, and wrote the manuscript draft. Y.C. and Y.L performed experiments and prepared figures. R.M. revised the manuscript. C.X. edited the manuscript. D.Y analyzed data. X.Z. performed Moso bamboo callus transformation. J.C conceived the project and edited the manuscript. M.Z. conceived the project, designed experiments and wrote the manuscript together.

ORCID

Long-Hai Zou https://orcid.org/0000-0001-5287-8139
Mingbing Zhou https://orcid.org/0000-0001-5674-4410
Jungnam Cho https://orcid.org/0000-0002-4078-7763

Data availability

The raw data of ALE-seq can be accessed under the project CNP0004168 in the China National GeneBank DataBase (CNGBdb). WGBS data and the associated transcriptomes were deposited in the National Center for Biotechnology Information under projects PRJNA826540, PRJNA828273, and PRJNA547876, and in the CNGBdb under project CNP0001319 and CNP0004168, respectively.

658 # Reference

659

Ayadi M, Delaporte V, Li Y-F, Zhou D-X. **2004**. Analysis of GT-3a identifies a distinct subgroup of trihelix DNA-binding transcription factors in *Arabidopsis*. *FEBS Letters* **562**: 147–154.

Bartels A, Han Q, Nair P, Stacey L, Gaynier H, Mosley M, Huang Q, Pearson J, Hsieh T-F, An Y-Q, *et al.* **2018**. Dynamic DNA Methylation in Plant Growth and Development. *International Journal of Molecular Sciences* **19**: 2144.

Baubec T, Finke A, Mittelsten Scheid O, Pecinka A. **2014**. Meristem-specific expression of epigenetic regulators safeguards transposon silencing in Arabidopsis. *EMBO reports* **15**: 446–452.

Bolger AM, Lohse M, Usadel B. **2014**. Trimmomatic: a flexible trimmer for Illumina sequence data. *Bioinformatics* **30**: 2114–2120.

Butelli E, Licciardello C, Zhang Y, Liu J, Mackay S, Bailey P, Reforgiato-Recupero G, Martin C. **2012**. Retrotransposons Control Fruit-Specific, Cold-Dependent Accumulation of Anthocyanins in Blood Oranges. *The Plant Cell* **24**: 1242–1255.

Canat A, Torres-Padilla M-E. **2021**. Retrotransposing a promoter for development. *Nature Cell Biology* **23**: 1221–1223.

Cho J, Benoit M, Catoni M, Drost H-G, Brestovitsky A, Oosterbeek M, Paszkowski J. **2018**. Sensitive detection of pre-integration intermediates of long terminal repeat retrotransposons in crop plants. *Nature Plants* **5**: 26–33.

Comfort N. **1999**. "The Real Point is Control": The Reception of Barbara McClintock's Controlling Elements. *Journal of the History of Biology* **32**: 133–162.

Daron J, Slotkin RK. **2017**. EpiTEome: Simultaneous detection of transposable element insertion sites and their DNA methylation levels. *Genome Biology* **18**: 91.

Demirer GS, Zhang H, Goh NS, González-Grandío E, Landry MP. **2019**. Carbon nanotube–mediated DNA delivery without transgene integration in intact plants. *Nature Protocols* **14**: 2954–2971.

Ding Y, Zou L-H, Ramakrishnan M, Chen Y, Zhu B, Yu L, Zhou M. **2024**. Abiotic stress-induced DNA methylation in transposable elements and their transcripts reveals a multi-layered response in Moso bamboo. *Industrial Crops and Products* **210**: 118108.

Ding Y, Zou L-H, Wu J, Ramakrishnan M, Gao Y, Zhao L, Zhou M. **2022**. The pattern of DNA methylation alteration, and its association with the expression changes of non-coding RNAs and mRNAs in Moso bamboo under abiotic stress. *Plant Science* **325**: 111451.

Drost H-G. **2020**. LTRpred: de novo annotation of intact retrotransposons. *Journal of Open Source Software* **5**: 2170.

Ewing AD, Gacita A, Wood LD, Ma F, Xing D, Kim M-S, Manda SS, Abril G, Pereira G, Makohon-Moore A, *et al.* **2015**. Widespread somatic L1 retrotransposition occurs early during gastrointestinal cancer evolution. *Genome Research* **25**: 1536–1545.

Feng J, Liu T, Qin B, Zhang Y, Liu XS. **2012**. Identifying ChIP-seq enrichment using MACS. *Nature Protocols* **7**: 1728–1740.

Galindo-González L, Mhiri C, Deyholos MK, Grandbastien M-A. **2017**. LTR-retrotransposons in plants: Engines of evolution. *Gene* **626**: 14–25.

Gao Z-M, Fan S-H, Gao J, Li X-P, Cai C-J, Peng Z-H. **2006**. Extract Genomic DNA from Phyllostachys edulis by CTAB-Based Method. *Forest Research* **19**: 725–728.

Gao Y, Ran L, Kong Y, Jiang J, Sokolov V, Wang Y. **2014**. Assessment of DNA methylation changes in tissue culture of *Brassica napus*. *Russian Journal of Genetics* **50**: 1186–1191.

Gaubert H, Sanchez DH, Drost H-G, Paszkowski J. **2017**. Developmental Restriction of Retrotransposition Activated in Arabidopsis by Environmental Stress. *Genetics* **207**: 813–821.

Ghosh A, Igamberdiev AU, Debnath SC. **2021**. Tissue culture-induced DNA methylation in crop plants: a review. *Molecular Biology Reports* **48**: 823–841.

Grandbastien M-A. **2015**. LTR retrotransposons, handy hitchhikers of plant regulation and stress response. *Biochimica et Biophysica Acta (BBA) - Gene Regulatory Mechanisms* **1849**: 403–416.

Griffiths J, Catoni M, Iwasaki M, Paszkowski J. **2018**. Sequence-Independent Identification of Active LTR Retrotransposons in Arabidopsis. *Molecular Plant* **11**: 508–511.

Gutzat R, Rembart K, Nussbaumer T, Hofmann F, Pisupati R, Bradamante G, Daubel N, Gaidora A, Lettner N, Donà M, *et al.* **2020**. Arabidopsis shoot stem cells display dynamic transcription and DNA methylation patterns. *The EMBO Journal* **39**: e103667.

Han Y, Wang X, Xu X, Gao Y, Wen G, Zhang R, Wang Y. **2018**. Responses of anti-oxidant enzymes and the ascorbate-glutathione cycle to heat, drought, and synergistic stress in *Phyllostachys edulis* seedlings. *Journal of Zhejiang A&F University* **35**: 268–276.

Hirochika H, Sugimoto K, Otsuki Y, Tsugawa H, Kanda M. **1996**. Retrotransposons of rice involved in mutations induced by tissue culture. *Proceedings of the National Academy of Sciences* **93**: 7783–7788.

Hirsch CD, Springer NM. **2017**. Transposable element influences on gene expression in plants. *Biochimica et Biophysica Acta (BBA) - Gene Regulatory Mechanisms* **1860**: 157–165.

Hu L, Li N, Zhang Z, Meng X, Dong Q, Xu C, Gong L, Liu B. **2019**. CG hypomethylation leads to complex changes in DNA methylation and transpositional burst of diverse transposable elements in callus cultures of rice. *The Plant Journal* **101**: 188–203.

Huettel B, Kanno T, Daxinger L, Aufsatz W, Matzke AJM, Matzke M. **2006**. Endogenous targets of RNA-directed DNA methylation and Pol IV in Arabidopsis. *The EMBO Journal* **25**: 2828–2836.

Jiang J, Liu J, Sanders D, Qian S, Ren W, Song J, Liu F, Zhong X. **2021**. UVR8 interacts with de novo DNA methyltransferase and suppresses DNA methylation in Arabidopsis. *Nature Plants* **7**: 184–197.

Jiang C, Mithani A, Gan X, Belfield EJ, Klingler JP, Zhu J-K, Ragoussis J, Mott R, Harberd NP. **2011**. Regenerant Arabidopsis Lineages Display a Distinct Genome-Wide Spectrum of Mutations Conferring Variant Phenotypes. *Current Biology* **21**: 1385–1390.

Kanazawa A, Liu B, Kong F, Arase S, Abe J. **2009**. Adaptive Evolution Involving Gene Duplication and Insertion of a Novel Ty1/copia-Like Retrotransposon in Soybean. *Journal of Molecular Evolution* **69**: 164–175.

Kimura Y, Tosa Y, Shimada S, Sogo R, Kusaba M, Sunaga T, Betsuyaku S, Eto Y, Nakayashiki H, Mayama S. **2001**. *OARE-1*, a Ty1-copia Retrotransposon in Oat Activated by Abiotic and Biotic Stresses. *Plant and Cell Physiology* **42**: 1345–1354.

Korotko U, Chwiałkowska K, Sańko-Sawczenko I, Kwasniewski M. **2021**. DNA Demethylation in Response to Heat Stress in Arabidopsis thaliana. *International Journal of Molecular Sciences* **22**: 1555.

Krueger F, Andrews SR. **2011**. Bismark: a flexible aligner and methylation caller for Bisulfite-Seq applications. *Bioinformatics* **27**: 1571–1572.

Kumar A, Bennetzen JL. **1999**. Plant Retrotransposons. *Annual Review of Genetics* **33**: 479–532.

Lanciano S, Carpentier M-C, Llauro C, Jobet E, Robakowska-Hyzorek D, Lasserre E, Ghesquière A, Panaud O, Mirouze M. **2017**. Sequencing the extrachromosomal circular mobilome reveals retrotransposon activity in plants. *PLOS Genetics* **13**: e1006630.

Langdon WB. **2015**. Performance of genetic programming optimised Bowtie2 on genome comparison and analytic testing (GCAT) benchmarks. *BioData Mining* **8**: 1.

Lee HY, Bahn SC, Kang Y-M, Lee KH, Kim HJ, Noh EK, Palta JP, Shin JS, Ryu SB. **2003**. Secretory Low Molecular Weight Phospholipase A2 Plays Important Roles in Cell Elongation and Shoot Gravitropism in Arabidopsis. *The Plant Cell* **15**: 1990–2002.

Lescot M, Déhais P, Thijs G, Marchal K, Moreau Y, Van de Peer Y, Rouzé P, Rombauts S. **2002**. PlantCARE, a database of plant cis-acting regulatory elements and a portal to tools for in silico analysis of promoter sequences. *Nucleic Acids Research* **30**: 325–327.

Lisch D. **2012**. How important are transposons for plant evolution? *Nature Reviews Genetics* **14**: 49–61.

Liu ZL, Han FP, Tan M, Shan XH, Dong YZ, Wang XZ, Fedak G, Hao S, Liu B. **2004**. Activation of a rice endogenous retrotransposon *Tos17* in tissue culture is accompanied by cytosine demethylation and causes heritable alteration in methylation pattern of flanking genomic regions. *Theoretical and Applied Genetics* **109**: 200–209.

Liu B, Kanazawa A, Matsumura H, Takahashi R, Harada K, Abe J. **2008**. Genetic Redundancy in Soybean Photoresponses Associated With Duplication of the Phytochrome A Gene. *Genetics* **180**: 995–1007.

Llorens C, Futami R, Bezemer D, Moya A. **2007**. The Gypsy Database (GyDB) of mobile genetic elements. *Nucleic Acids Research* **36**: D38–D46.

Love MI, Huber W, Anders S. **2014**. Moderated estimation of fold change and dispersion for RNA-seq data with DESeq2. *Genome Biology* **15**: 550.

Makarevitch I, Waters AJ, West PT, Stitzer M, Hirsch CN, Ross-Ibarra J, Springer NM. **2015**. Transposable Elements Contribute to Activation of Maize Genes in Response to Abiotic Stress. *PLoS Genetics* **11**: e1004915.

Martínez G, Slotkin RK. **2012**. Developmental relaxation of transposable element silencing in plants: functional or byproduct? *Current Opinion in Plant Biology* **15**: 496–502.

Matsunaga W, Kobayashi A, Kato A, Ito H. **2011**. The effects of heat induction and the siRNA biogenesis pathway on the transgenerational transposition of ONSEN, a copia-like retrotransposon in Arabidopsis thaliana. *Plant and Cell Physiology* **53**: 824–833.

Miyao A, Nakagome M, Ohnuma T, Yamagata H, Kanamori H, Katayose Y, Takahashi A, Matsumoto T, Hirochika H. **2011**. Molecular Spectrum of Somaclonal Variation in Regenerated Rice Revealed by Whole-Genome Sequencing. *Plant and Cell Physiology* **53**: 256–264.

Modzelewski AJ, Shao W, Chen J, Lee A, Qi X, Noon M, Tjokro K, Sales G, Biton A, Anand A, *et al.* 2021. A mouse-specific retrotransposon drives a conserved Cdk2ap1 isoform essential for development. *Cell* **184**: 5541-5558.e22.

Neph S, Kuehn MS, Reynolds AP, Haugen E, Thurman RE, Johnson AK, Rynes E, Maurano MT, Vierstra J, Thomas S, *et al.* 2012. BEDOPS: high-performance genomic feature operations. *Bioinformatics* **28**: 1919–1920.

Nie Q, Qiao G, Peng L, Wen X. **2019**. Transcriptional activation of long terminal repeat retrotransposon sequences in the genome of pitaya under abiotic stress. *Plant Physiology and Biochemistry* **135**: 460–468.

Noshay JM, Anderson SN, Zhou P, Ji L, Ricci W, Lu Z, Stitzer MC, Crisp PA, Hirsch CN, Zhang X, *et al.* 2019. Monitoring the interplay between transposable element families and DNA methylation in maize. *PLOS Genetics* **15**: e1008291.

Paterson AH, Bowers JE, Bruggmann R, Dubchak I, Grimwood J, Gundlach H, Haberer G, Hellsten U, Mitros T, Poliakov A, *et al.* 2009. The *Sorghum bicolor* genome and the diversification of grasses. *Nature* **457**: 551–556.

Quinlan AR, Hall IM. **2010**. BEDTools: a flexible suite of utilities for comparing genomic features. *Bioinformatics* **26**: 841–842.

Ramakrishnan M, Papolu PK, Mullasseri S, Zhou M, Sharma A, Ahmad Z, Satheesh V, Kalendar R, Wei Q. **2022**. The role of LTR retrotransposons in plant genetic engineering: how to control their transposition in the genome. *Plant Cell Reports* **42**: 3–15.

Ramakrishnan M, Yrjälä K, Vinod KK, Sharma A, Cho J, Satheesh V, Zhou M. **2020**. Genetics and genomics of moso bamboo (*Phyllostachys edulis*): Current status, future challenges, and biotechnological opportunities toward a sustainable bamboo industry. *Food and Energy Security* **9**: e229.

Sabot F, Picault N, El-Baidouri M, Llauro C, Chaparro C, Piegu B, Roulin A, Guiderdoni E, Delabastide M, McCombie R, *et al.* 2011. Transpositional landscape of the rice genome revealed by paired-end mapping of high-throughput re-sequencing data. *The Plant Journal* **66**: 241–246.

Schorn AJ, Gutbrod MJ, LeBlanc C, Martienssen R. **2017**. LTR-Retrotransposon Control by tRNA-Derived Small RNAs. *Cell* **170**: 61–71.

Skorupa M, Szczepanek J, Mazur J, Domagalski K, Tretyn A, Tyburski J. **2021**. Salt stress and salt shock differently affect DNA methylation in salt-responsive genes in sugar beet and its wild, halophytic ancestor. *PLOS ONE* **16**: e0251675.

Steinbiss S, Willhoeft U, Gremme G, Kurtz S. **2009**. Fine-grained annotation and classification of de novo predicted LTR retrotransposons. *Nucleic Acids Research* **37**: 7002–7013.

Tao G-Y, Ramakrishnan M, Vinod KK, Yrjälä K, Satheesh V, Cho J, Fu Y, Zhou M. **2020**. Multi-omics analysis of cellular pathways involved in different rapid growth stages of moso bamboo. *Tree Physiology* **40**: 1487–1508.

Tsukahara S, Kobayashi A, Kawabe A, Mathieu O, Miura A, Kakutani T. **2009**. Bursts of retrotransposition reproduced in Arabidopsis. *Nature* **461**: 423–426.

Varet H, Brillet-Guéguen L, Coppée J-Y, Dillies M-A. **2016**. SARTools: a DESeq2- and edgeR-based R pipeline for comprehensive differential analysis of RNA-Seq data. *PLoS ONE* **11**: e0157022.

Waititu JK, Zhang C, Liu J, Wang H. **2020**. Plant Non-Coding RNAs: Origin, Biogenesis, Mode of Action and Their Roles in Abiotic Stress. *International Journal of Molecular Sciences* **21**: 8401.

Wang X, Cnops G, Vanderhaeghen R, De Block S, Van Montagu M, Van Lijsebettens M. **2001**. *AtCSLD3*, A Cellulose Synthase-Like Gene Important for Root Hair Growth in Arabidopsis. *Plant Physiology* **126**: 575–586.

Wang L, Shi Y, Chang X, Jing S, Zhang Q, You C, Yuan H, Wang H. **2018**. DNA methylome analysis provides evidence that the expansion of the tea genome is linked to TE bursts. *Plant Biotechnology Journal* **17**: 826–835.

Wei L, Xiao M, An Z, Ma B, Mason AS, Qian W, Li J, Fu D. **2013**. New Insights into Nested Long Terminal Repeat Retrotransposons in Brassica Species. *Molecular Plant* **6**: 470–482.

Wright SI, Agrawal N, Bureau TE. **2003**. Effects of Recombination Rate and Gene Density on Transposable Element Distributions in *Arabidopsis thaliana*. *Genome Research* **13**: 1897–1903.

Xiao DC, Zhang ZJ, Xu YW, Yang L, Zhang FX, Wang CL. **2013**. Cloning and functional analysis of *Phyllostachys edulis* MYB transcription factor PeMYB2. *Hereditas (Beijing)* **35**: 1217–1225.

Yamazaki H, Tasaka M, Shikanai T. **2004**. PPR motifs of the nucleus-encoded factor, PGR3, function in the selective and distinct steps of chloroplast gene expression in *Arabidopsis*. *The Plant Journal* **38**: 152–163.

Ying YQ, Wei JF, Xie NN, Jiang Q, Fang W. **2011**. Effects of natural low temperature stress on physiological and biochemical properties of *Phyllostachys edulis*. *Journal of Nanjing Forestry University* **32**: 133–136.

Zhang WH, Chen Q. **2011**. Study on Regularity of Growth and Decay of Surface Free Radical of the Moso Bamboo After UV-birradiation. *Surface Technology* **40**: 65–67.

Zhao H, Gao Z, Wang L, Wang J, Wang S, Fei B, Chen C, Shi C, Liu X, Zhang H, *et al.* 2018. Chromosome-level reference genome and alternative splicing atlas of moso bamboo (*Phyllostachys edulis*). *GigaScience* **7**: 1–12.

Zheng H, Ji H, Jiang Z-Q, Xu Z-X, Zhou M-B. **2019**. Identification and Transcription Activity Analysis of a Full-length LTR Retrotransposon of PHRE9 in Moso Bamboo (*Phyllostachys edulis*). *Journal of Agricultural Biotechnology* **27**: 645–655.

Zhou M, Hu B, Zhu Y. **2017a**. Genome-wide characterization and evolution analysis of long terminal repeat retroelements in moso bamboo (*Phyllostachys edulis*). *Tree Genetics & Genomes* **13**: 43.

Zhou M, Liang L, Hänninen H. **2018**. A transposition-active *Phyllostachys edulis* long terminal repeat (LTR) retrotransposon. *Journal of Plant Research* **131**: 203–210.

Zhou M, Zhou Q, Hänninen H. **2017b**. The distribution of transposable elements (TEs) in the promoter regions of moso bamboo genes and its influence on downstream genes. *Trees* **32**: 525–537.

660

661

Supporting Information

Fig. S1 Clustering analysis for sample reproducibility based on eclDNA abundance.

Fig. S2 Validation of the eclDNA abundance of 22 potentially active LTR retrotransposons in moso bamboo by qPCR.

Fig. S3 Validation of the transcriptional levels of 22 potentially active LTR retrotransposons in moso bamboo by qPCR.

Fig. S4 GO function enrichment analysis of 2,104 genes. (a) cell component; (b) molecular function; (c) biological process.

Fig. S5 GO enrichment analysis of the adjacent protein-coding genes near new insertions of LTR-REs in UV and Salt samples (a) and *PHRE11* and *PHRE12* (b).

Fig. S6 Sequence structure of two active LTR retrotransposons in moso bamboo.

Fig. S7 Detection of *HygR* gene of T1, T2, and T3 generation of transgenic *A. thalian*a.

Fig. S8 RT-PCR analysis of *HygR* gene expression in the transgenic moso bamboo calli.

Table S1 Primers for ALE-seq library preparation.

Table S2 Primers for identification of *PHRE11*'s and *PHRE12*'s new insertion sites with TD technology.

Table S3 Primers of amplification of *PHRE11*.

Table S4 Primers of amplification of HygR gene integrated into PHRE11 in transgenic Moso bamboo and *A. thaliana*.

Table S5 Primers for PHRE11 copy number analysis in *A. thaliana*.

Table S6 Specific primers from HygR used for chromosome walking.

Table S7 Primers for eclDNA qPCR validation.

Table S8 Primers for RNA qPCR validation.

Table S9 Frequency of PBS present in LTR retrotransposons of Moso bamboo.

Table S10 Information of 2,170 activated LTR retrotransposons.

Table S11 Top twenty-two most significantly up-regulated LTR retrotransposons in ICD, Calli, Salt and UV samples.

Table S12 Cis-element identification of the LTR regions of the 2170 activated LTR-Res.

Table S13 KEGG Pathway enrichment analysis of 2,014 genes.

Table S14 PHRE11's new insertion sites in *A. thaliana* genome.

Table S15 New insertions of PHRE11 and adjacent gene information in transgenic Moso bamboo calli.